Mediterranean Archaeology and Archaeometry, Vol. 2010, No. 4, pp. 61-67

TL AND OSL RESPONSE OF TURQUOISE FOR DOSIMETRIC APPLICATION

B. Subedi[1,2,3], D. Afouxenidis[1,2], G.S. Polymeris[1,4], N.C. Tsirliganis[1], K.M. Paraskevopoulos[3], G. Kitis[2]

[1]Archaeometry Laboratory, Cultural and Educational Technology Institute (C.E.T.I.), R.C. "Athena", Tsimiski 58, GR-67100, Xanthi, Greece

[2]Nuclear Physics Laboratory, Department of Physics, Aristotle University of Thessaloniki, GR54124, Thessaloniki Greece

[3]Physics Department, Solid State Section, Aristotle University of Thessaloniki, 54124 Thessaloniki, Greece

[4] IŞIK University, Faculty of Science and Arts, Physics Department, 34980-Sile, Istanbul, Turkey

Corresponding author: bsubedi@physics.auth.gr

ABSTRACT

Turquoise is one of the amongst first gem stones used in jewelry and possessing cultural value since 2000 BC (at least). This work attempts characterize this stone scientifically using both thermally (TL) and optically stimulated luminescence (OSL) techniques. The experimental investigation included 1) the study of the natural TL and OSL signals, 2) the reproducibility of TL sensitivity over repeated irradiation and TL readout cycles, 3) dependence of sensitivity on annealing temperatures and 4) the TL and OSL dose response curves. The potential use of the TL and OSL techniques in determination of provenance, accidental dosimetry and probably to authenticity and dating purposes are then discussed.

KEYWORDS: Turquoise gemstone, TL and OSL, Luminescence, dose response, accidental dosimeter, authenticity and dating

INTRODUCTION

One of the oldest non-transparent gemstones, turquoise, has been in use in eastern, middle-eastern and western culture for a long time. Its considerable strength (hardness 5-6) and existence in multi-color; sky blue, dark blue and even in yellowish were its positive side to use in ancient artifacts and ornaments, decoration of souvenir items. Additionally, it has been used as a source for replication of color to modern appliances and even in modern gemstone therapy, Ishaque et al., 2009. Turquoise has been well characterized by spectroscopy techniques Hunt et al., 1972 and by ESR and EPR (Diaz et al., 1971; Clark et al., 1979; Sharma et al., 1988). Spectroscopy technique was further used by Frost et al, 2006 to study molecular spectra of turquoise of different origins. Turquoise is associated with minerals such as pyrite, quartz, chert, magnesium oxide, apatite, chalcopyrite, chalcedony and clays. From the TL dating point of view, chert, quartz, and chalcedony constitute basic components for the dating of Paleolithic geo-archaeological sites, with ages beyond the upper limit of radiocarbon (generally about 40.000 years), Martini et al 2001. Hull et al, 2006 studied the turquoise using its hydrogen and cupper isotope for the provenance study. Unfortunately, only limited attempts have been made for the study of provenance and characterization of turquoise, (Hull et al, 2007, Mathien, 2001).

Recently a luminescence study of turquoise and its physicochemical characteristics were reported by Crespo-Feo et al, 2009. These authors identified its association with quartz and different phosphates (fluorapatite, monacite and xenotime). They also discovered its morphological changes due to compositional variations of substitution cations in Cu^{+2} and Al^{3+} through XRD and SEM analyses. The aim of this work is to perform a TL/OSL characterization of this material and to examine its potential use in retrospective dosimetry and probably in authenticity and provenance.

EXPERMENTAL PROCEDURES

Turquoise gemstone (greenish blue) was crushed after scarping incrustation of dirt, sieved to get grains of size between 20-80 μm for measurements and each sample mass was selected as 6mg. Mass of the sample was spread in thin layer on stainless steel disk of 1cm² diameter. The TL and OSL measurements were performed using the RISØ TL/OSL reader (model TL/OSL–DA–15) equipped with a high-power blue LED light source, and a 0.078Gy/s $^{90}Sr/^{90}Y$ β source dose rate (Bøtter-Jensen et al, 2000). The reader was fitted with a 9635QA PM Tube. The detection optics consisted of a 7.5 mm Hoya U-340 (λ_{p} ~340 nm, FWHM 80 nm) filter. Blue light stimulation for OSL was achieved using LEDs (470 nm, FWHM 20 nm) delivering up to 36 mW/cm² at the sample position. The CW-OSL measurements were performed at 90% power and stimulation duration 500s. In LM–OSL measurements, the ramping rate was 0.04 mW/cm²/s (end power 100%) and stimulation duration 500s. All TL measurements were performed using a heating rate of 1 °C/s in order to avoid significant temperature lag, the temperature difference between the heater plate and the sample. The sample processing was done under dark room to control presence light sources.

RESULTS AND DISCUSSION

Natural TL and OSL signal

Figs.1 and 2 show the natural TL recorded up to 773K and natural LM-OSL measured in stimulation power between zero to 100% (36mW/cm²), using blue LED light as source accordingly. All measurements of natural TL, natural LM-OSL at both room temperature and at 125^{0}C (393K) showed presence of numbers of peaks. Natural signals of TL infer strong TL signal starting from 500K along with number of low and high temperature peaks.

Glow Curve analysis

In the present work all TL glow curves of both un-annealed and annealed were analyzed by a computerized glow curve de-convolution (CGCD) technique using general order kinetics (Kitis et al., 1998). The goodness of the fir was tasted by the Figure of merits (FOM) defined by Balian and Eddy (1977). Characteristic examples of analyzed glow curves of both un-annealed

and annealed samples, are shown in Fig. 3 (A) and Fig. 3 (B) respectively.

Sensitivity versus irradiation-readout cycle

A very important step in the characterization procedure is to examine the sensitivity of the material as a function of successive irradiation-readout cycles. The reason is that in the case the sensitivity is stable, then the use of single aliquot protocols are favored. Fig. 4 shows the sensitivity of the un-annealed samples versus irradiation-readout cycles normalized over the sensitivity of the first cycle using a test dose, 2.5Gy. This behavior concerns all the TL glow-peaks shown in Fig.3(A). In fact, the sensitivity increases by a factor 1,5 up to 5th cycle it means that single aliquot protocols have to be used carefully.

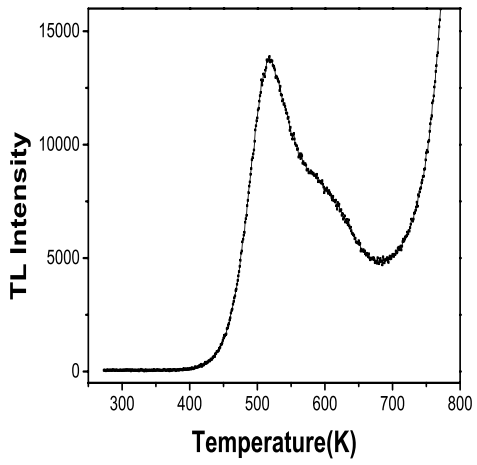

Figure 1. Natural TL glow curve up to 773K

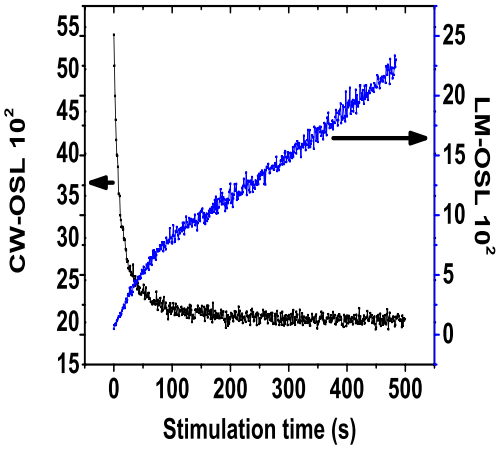

Figure 2. Natural CW-OSL and LM-OSL at room temperature, arrows head indicates the curves corresponding to the axis of CW-OSL and LM-OSL.

In the case of samples annealed at 773K, 873K, 973K, 1073K and 1173K the characteristic glow curve shape is shown in Fig. 3(B). This glow-curve contains a clear glow peaks at 345 K as well as a system of three glow-peaks centered at about 501K. For the dosimetric application only the 431-625K peak region seems to be of interest. However, the behavior of both the TL glow-peaks regions is studied. The results are shown in Fig. 5. It is observed that the sensitivity versus irradiation-readout cycle of all TL peaks is more or less stable. Namely, the variation in the dosimetric peak integral was less than ±5%.

Sensitivity and annealing temperature

Another basic characterization property is the variation of the sensitivity as a function of annealing temperature. The sensitivity of each annealed sample was tested using the following sequence (for single aliquot);

Annealed sample +Dose (D_i) $\rightarrow$TL, where D_i=2.5, 5, 10, 20, 40 and 2.5 Gy. The last dose of the sequence being equal to the first dose aims to detect some pre-dose effect. On the other hand this procedure is similar to the recycling ratio step which was established in the framework of the Single Aliquot Regenerative (SAR) protocol of Murray and Wintle (2000). Practically small variation in integral can be monitored from one aliquot to another even in identical samples under the identical condition during TL readouts. In order to cope with this fact, 7% possible experimental error was included on each one of the evaluated peak integrals, based on the respective glow curves. The results are shown in Fig. 6. The solid square symbol indicates integral with the initial dose of 2.5Gy, whereas the solid circles symbol corresponds to the sensitivity of the final dose of 2.5Gy (see sequence above). The results of Fig.6 are two-fold. (1) The sensitivity is increases from 773K to 1073 by a factor of about 4 and decreases at 1173K. (2) There is a systematic slight increase of the sensitivity due to the pre-dose at each annealing temperature.

TL dose response

TL dose response was investigated for both un-annealed and annealed samples in the dose

region up to 512Gy and 40Gy respectively. The nature of the annealed glow curve is shown in Fig. 3. The measurements of the un-annealed samples were performed after erasing its naturally occurring signal by a TL readout up to 773K at 1K/s. The results of CGCD analysis for un-annealed samples are presented in Fig. 7. The analysis resulted 6 peaks with peak maximum temperature as T_{max1} =348.38±1.5K, T_{max2}=375±2K, T_{max3}=410±2.5K, T_{max4}=451±3K, T_{max5}=496±1K, and T_{max6}=751±22K. It was also observed from every glow curve deconvolution analysis the value of FOM was less than 2%.

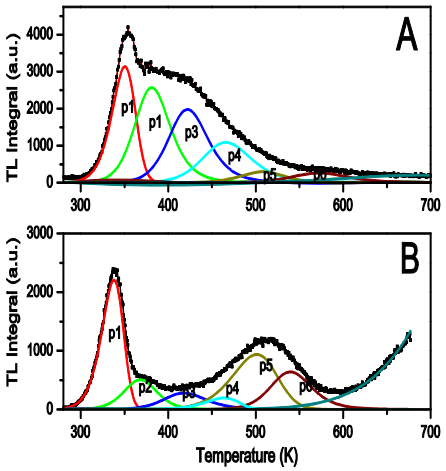

Figure 3. Examples of glow curves de-convolution (A) un-annealed sample (using dose 512Gy) and (B) annealed sample with 20Gy. Identified peaks are represented by P1, P1, P3, P4, P5 and P6 in both cases. Lines with symbols (thick) are experimental glow curves.

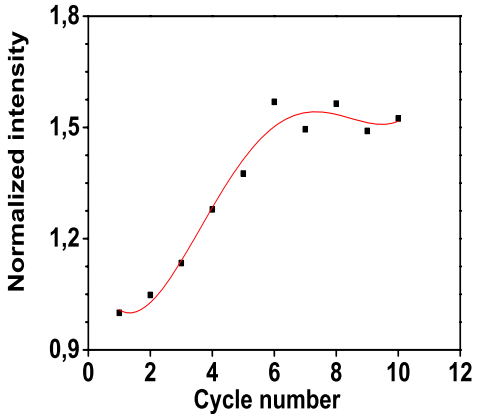

Figure 4. Normalized integral versus number of successive cycles with dose 2.5Gy (unannealed) from temperature region (273-467)K, symbol represents the experimental points and solid line is 4th order polynomial fit.

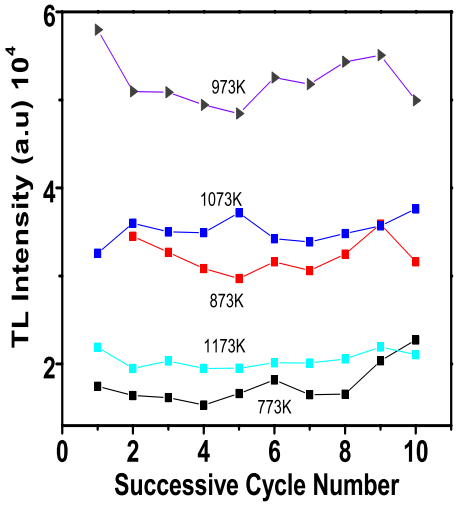

Figure 5. TL intensity of higher temperature region with number of successive cycles using same dose for samples annealed at different temperature.

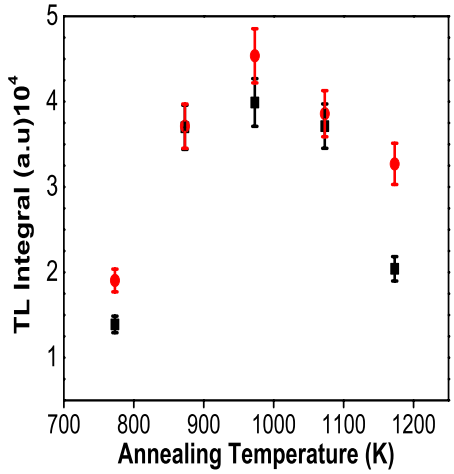

Figure 6. Sensitivity as a function of annealing temperature with test dose, symbol square and round indicates integral in initial and final stage respectively (in the integral region 430-625K).

The low temperature TL peaks P_1, P_2 and P_3 showed a linear dose response from the lowest dose whereas the high temperature TL peaks p_4 and P_5 showed a slight sub-linearity at low doses followed by linearity at higher doses.

The results concerning the annealed samples are shown in Figure.8 for the low temperature TL peaks and Figure.9 for the high temperature TL peaks. The doses used were 2.5Gy, 5Gy, 10Gy, 20Gy, and 40Gy. It infers linearity with dose greater than 2Gy.

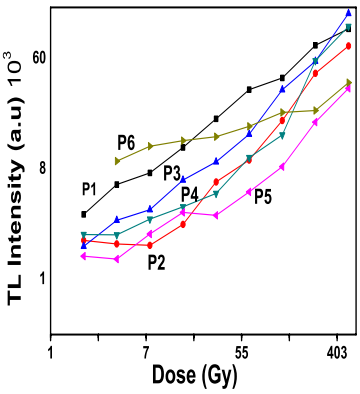

Figure 7. Integral obtained from de-convolution analysis of the TL glow curves from doses 1Gy, 2Gy, 4Gy, 8Gy, 16Gy, 32Gy, 64Gy, 128Gy, 256Gy and 512Gy. P1, P2, P3, P4, P5 and P6 stand for 6 different peaks integrals, both axes are expressed in ln scale in order to see clearly.

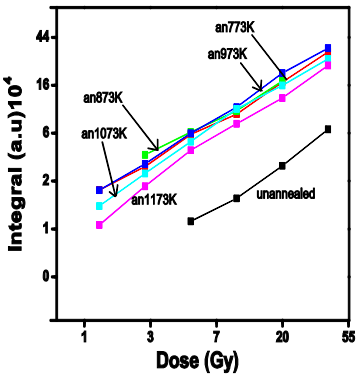

Figure 8. TL dose response for low temperature peak integral in the temperature region (280-430) K on all annealed samples, both axis are in log scale in order to see clearly.

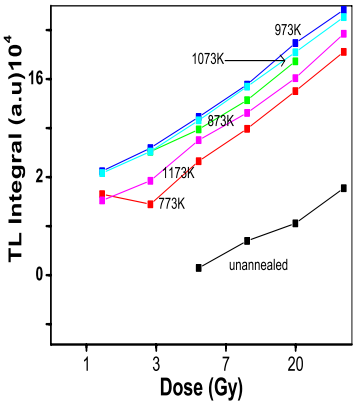

Figure 9. TL dose response for high temperature peak integral in the temperature region (431-625) K for annealed samples of five different temperature, both axis are in log scale.

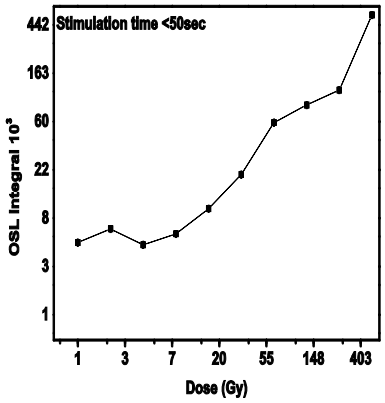

Figure 10. Dose response of OSL curves for doses: 1Gy, 2Gy, 4Gy, 8Gy, 16Gy, 32Gy, 64Gy, 128Gy, 256Gy and 512Gy in lower stimulation time up to 50 sec including 7% experimental error, both axes are in ln scale.

OSL dose response

The OSL dose response curve was preformed in the same dose region as that of TL dose response for unannealed sample after erasing the natural signal by heating to 773K. The OSL decay curves were analyzed with stimulation times of 0-50s and 50-500s and corresponding dose response is plotted in Figs 10 and 11. In the lower stimulation time integrals were plotted with dose only after subtracting their background. Both the integral regions were analyzed including experimental error 7% and they were plotted with the function of applied doses.

It revealed that both integral have same behavior with applied doses; presence of sublinearity at low doses (up to 4Gy), which is followed by linearity up to the highest delivered dose in each case.

Another important property of any material to use as a dosimeter is its lowest detectable limit (LDL). The LDL is defined as the dose which results in TL/OSL intensity three times the standard deviation of the background signal. We have calculated the LDL for both as-is and annealed samples. For safeness we took into account 10 times for standard deviation. So the LDL was 2Gy for as-is and 0.5Gy for annealed.

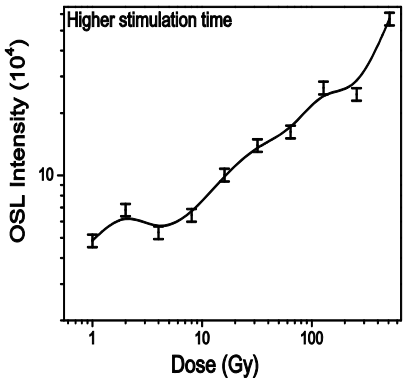

Figure 11. Dose response of OSL curves for doses: 1Gy, 2Gy, 4Gy, 8Gy, 16Gy, 32Gy, 64Gy, 128Gy, 256Gy and 512Gy in stimulation time 51 to 500 sec. (both axis are in log scale)

CONCLUSION

Linearity with dose is obtained by both TL and OSL above 4Gy over a wide range of doses. Stable integral of peaks of glow curve were found with repeated cycle of dose measurement in both the case of annealed and un-annealed samples. De-convolution of the glow curves divulge the presence of 6 peaks within the region of (273-773)K. Experimental results further suggest that turquoise can be used for accidental dosimeter and probably for authenticity testing, but it should be investigated in more detail for its other crucial parameters such as fading, bleaching ability to support for the later two purposes. Since the composition of turquoise depends upon the number of phosphate group, hydroxyl groups, Cu, Al, Zn, and Cr ions, the composition of these basic components can be different from one mine of turquoise to another. In the same way the minerals which are associated with turquoise can also influence the nature of the glow curves, as well as other luminescence features, such as sensitivity of the peaks. However, more research is required based on geological locations and sample types. In the present stage, this study can pave a way directly towards its potential use for provenance research.

REFERENCES

Balian, H.G. and Eddy, N.W. (1977). Figure of Merit (FOM), an improved Criterion over the normalised Chi-squared Test for assessing Goodness-of-fit of Gamma Ray Spectra Peaks. *Nuclear Instrum. Methods* 145, 389-395.

Belik, H.G., Ciftci, M., 2008. Cathoathodoluminescence properties of turquoise.C.B.U.J. Sci. 42, 195–2000.

Bøtter-Jensen, Bulur, E., Duller, G.A.T. and Murray A.S. (2000). Advances in luminescence instrument systems. *Radiation Measurements 32, 523–528.*

Bøtter-Jensen Lars, Mckeever Stephen W.S., Wintle A. G., (2003). Optically Stimulated Luminescence Dosimetry. *Elsevier Publishing, Amsterdam*.

Crespo-Feo, E., Garcia-Guinea J., Correcher V., Prado-Herrero P., Can N, (2010) Luminescence Behavior of $CuAl_6(PO_4)_4(OH)_8.4H_2O$. *Radiation Measurements* 45, 749–752.

Chen Reuven, McKeever Stephen W.S.,(1997). Theory of thermoluminscence and related phenomena, *World Scientific*.

Chen, R. and Kirsh, Y., (1981). Analysis of thermally stimulated processes, *Pergamon Press, London/ Oxford.*

Clark, C.O., Poole, C.P., Farach, H.A., (1979). Variable-temperature electron spins resonance of turquoise. *Am. Mineral*. 64, 449–451.

Diaz, J., Farach, H.A., Poole Jr., C.P., (1971). An electron spins resonance and optical study of turquoise. *Am. Mineral*. 56, 773–781.

Glen Akridge D. and Paul H. Benoit, (2001). Luminescence properties of chert and some archaeological applications, *Journal of Archaeological Science* 28, 143–151.

Hull Sharan, Fayek Mostafa, Joan Frances, Mathien, Phillip Shelley, Kathy Roler Durand, (2008). A new approach to determining the geological provenance of turquoise artifacts using hydrogen and copper stable isotopes, *Journal of Archaeology science* vol.35, No 5,1355-136.

Ishaque S., Saleem T., Qidwai W., (2009). Knowledge, attitudes and practices regarding gemstone therapeutics in a selected adult population in Pakistan, *BMC Complementary and Alternative Medicine* 2009, 9:32doi:10.1186/1472-6882-9-32.

Kitis, G., Gomez-Ros, J.M. and Tuyn J.W.N, (1998). Thermoluminescence glow-curve deconvolution functions for first, second and general orders of kinetics, *Journal of Phys. D: Appl. Phys*. 31, 2636–2641.

Martini Marco, Emanuela Sibilia, Silvia Croci and Mauro Cremaschi, (2001). Thermoluminescence (TL) dating of burnt flints: problems, perspectives and some examples of application, *Journal of Heritage*, Vol 2, Issue3, 179-190.

Murr, L.E., 1979. An electron microscopic study of crystalline turquoise. *Journal of Material. Science.* 14, 490–493.

Murray A.S., Wintle A.G. (2000). Application of the single-aliquot regenerative-dose protocol to the 3758C quartz TL signal. *Radiation Measurements* 32, 579-583.

Powell, Eric A. "The Turquoise Trail" (2005). *Archaeology*, Vol. 58, No.1.

Ray L. Frost, B. Jagannadha Reddy, Wayde N. Martens, Matt Weier, (2006). The molecular structure of the phosphate mineral turquoise—a Raman spectroscopic study, *Journal of Molecular Structure*, No 788, 224–231.

Sharma, K.B.N., Moorthy, L.R., Reedy, B.J., Vedanand, S., (1988). EPR and electronic absorption spectra of copper bearing turquoise mineral. *Physycs Lett. A* 132, 293–297.